Journal of Plant Pathology
https://doi.org/10.1007/s42161-026-02330-9

ORIGINAL ARTICLE

Morphological and molecular identification of *Magnaporthe oryzae* causing finger millet blast disease in Kenya

Angeline N. Wambua[1,2] · Evans N. Nyaboga[2] · Millicent Avosa[1] · Matthews M. Dida[3] · Henry F. Ojulong[1] · Benjamin Kilian[4] · Edward K. Muge[2] · Sheillah Cheroitich[5] · Damaris A. Odeny[1]

Received: 17 April 2026 / Accepted: 29 September 2026
© The Author(s) 2026

Abstract
Finger millet {*Eleusine coracana* (L.) Gaertn.} is an underutilized climate-resilient cereal crop with excellent nutraceutical properties. It is an important subsistence crop to the majority smallholder women farmers in western and eastern parts of Kenya, where it is grown under low input mixed cropping systems. One of the challenges limiting its production is blast disease caused by *Magnaporthe oryzae* (syn. *Pyricularia oryzae*). The objective of this study was to identify and characterize *M. oryzae* isolates associated with finger millet blast disease in Kenya. A field survey was undertaken across seven major finger millet growing counties resulting in the collection of 450 symptomatic tissues from leaf, neck and finger. Monoconidial cultures of 93 isolates were characterized using morphological and molecular methods. Pathogenicity tests were performed using two distinct isolates across 18 diverse finger millet genotypes. Morphological analysis grouped the isolates into two major clades that were neither based on tissue type nor geographical location. *ITS5/4* identified 46 isolates as *M. oryzae*, 28 of which were further validated using *Pot2a*, and another 18 using *Pfh2* primers. Distinct isolates S2_N_BS from the neck and S72_F_HM from finger tissue elicited different host responses suggesting genetic differences in host genotypes to the two isolates. The findings from the present study add knowledge for future morphological and molecular identification of *M. oryzae* isolates and further suggests the presence of different pathotypes that will need to be characterized in the future.

Keywords *Eleusine coracana* · *Magnaporthe oryzae* · ITS5/4 · Pfh2 · Pot2a

Introduction

Finger millet {*Eleusine coracana* (L.) Gaertn.; 2n = 4x = 36} is a cereal crop cultivated in the arid and semi-arid regions of Africa and Asia (Odeny et al. 2020; Zhang et al. 2019). Believed to have been domesticated around the highlands of Ethiopia and Uganda (Hilu and De Wet 1976), finger millet remains the most important millet in East Africa. In Kenya, finger millet production is mainly done by smallholder women farmers under low input mixed cropping systems. Despite the promising benefits, its productivity remains low with yields ranging between 500 and 750 kg/ha compared to a potential 2,500 kg/ha (Grovermann et al. 2018). The low productivity is mainly attributed to biotic and abiotic stresses (Odeny et al. 2020), and the high labor demand due to lack of mechanization.

Among the biotic stresses, blast disease caused by the heterothallic ascomycete, *Pyricularia oryzae* Cavara, synonym *Magnaporthe oryzae* B. C. Couch (Takan et al. 2012) is the most devastating. The same fungus also parasitizes a wide range of other economically important cereals such as rice (*Oryza sativa* L.), wheat (*Triticum aestivum*), foxtail millet (*Setaria italica*) and their relatives (Aravind et al. 2022; Noman et al. 2022). Neck and finger blast are the

✉ Damaris A. Odeny
damaris.odeny@icrisat.org

1 International Crops Research Institute for the Semi-Arid Tropics (ICRISAT), P.O. Box 39063, Nairobi 0063, Kenya

2 Department of Biochemistry, University of Nairobi, P.O. Box 30197, Nairobi 00100, Kenya

3 Maseno University, Private Bag, Maseno 40105, Kenya

4 Global Crop Diversity Trust, Platz der Vereinten Nationen 7, 53113 Bonn, Germany

5 Department of Entomology and Nematology, University of Florida, 1881 Natural Area Drive, Steinmetz Hall, Gainesville, FL 32611, USA

Published online: 27 October 2026

most destructive forms in finger millet causing poor and/or no grain filling (Manyasa et al. 2019). Losses attributed to finger millet blast disease can be as high as 90% under favorable weather and host genotype susceptibility (Ekwamu 1991; Rao 1990). Individual strains of *M. oryzae* are host genus-specific and have been classified into distinct pathotypes according to their pathogenicity. *Eleusine* pathotypes infect finger millet, *Setaria* pathotypes infect foxtail millet, *Oryza* pathotypes infect rice (*Oryza sativa* L.) and *Triticum* pathotypes infect wheat (Kato et al. 2000). Although there are several reports on the morphological and molecular characterization of pathotypes of *M. oryzae Triticum* (*MoT*) (Pereira et al. 2014; Tembo et al. 2020; Kang et al. 2021) and *M. oryzae Oryzae* (*MoO*) (Abed-Ashtiani et al. 2016; Gowda et al. 2015; Muni and Nadarajah 2014; Sahu et al. 2018), limited studies have been undertaken to characterize *M. oryzae Eleusine* (*MoE*) pathotypes in Kenya and East Africa (Takan et al. 2012).

Crop diversification and structure are known to influence the emergence and evolution of plant pathogens (Gladieux et al. 2010; Saleh et al. 2014). There are significantly fewer studies characterizing *M. oryzae Eleusine* in general, but even much fewer in East Africa, the center of finger millet diversity. A previous characterization done more than a decade ago for isolates from Kenya and Uganda revealed specific host adaptation for western Kenyan isolates, although the study was not conclusive with respect to population structure and genetic diversity (Takan et al. 2012). Genetic diversity and molecular studies on plant-pathogen interactions are extremely important in enhancing our understanding of pathogen infection strategies and the elicited plant defense mechanisms (Dodds and Rathjen 2010). A better understanding of the diversity of finger millet blast fungal isolates will be important in breeding for improved blast resistance (Xing et al. 2017) in East Africa.

The main objective of this study was to use a combination of morphological and molecular analysis (*ITS5/4*, *Pot2a* and *Pfh2*) to identify *M. oryzae* isolates associated with finger millet blast in major production regions of Kenya. The non-coding internal transcribed spacer (*ITS*) of ribosomal RNA genes is well known as a universal fungal gene (Schoch et al. 2012). It is a widely useful molecular tool for the identification and genetic diversity analysis of different fungal species (Chen et al. 2021). *Pot2a* and *Pfh2* have been reported to be specific to the blast pathogen (*M. oryzae*) and have been successfully used in *M. oryzae* identification in perennial ryegrass (*Lolium perenne* L.), rice and wheat (Harmon et al. 2003; Pieck et al. 2017). The *Pot2* transposon occurs in multiple copies throughout the genome of *M. oryzae* (Kachroo et al. 1994) which enhances the probability of amplification and detection.The variation in pathogenicity of selected isolates was further established by testing two distinct isolates against a differential set of 18 cultivars.

Materials and methods

Collection of diseased finger millet plant material

Field surveys were performed across major finger millet growing counties of Makueni (MK), Homabay (HM), Kisii (KS), Kisumu (MS), Busia (BS), Nyamira (NY) and Migori (MG) (Fig. 1) during the rainy seasons in 2019, 2021 and 2022. A total of four hundred and fifty (450) symptomatic finger millet samples were collected (Supplementary Table S1) from research stations and farmers' fields for analysis. The samples with typical blast lesions were collected from leaves, neck and fingers. The infected leaves showed diamond-shaped lesions with black or brown outer lining, the neck showed black/brown necrotic lesions, while symptomatic fingers presented black/brown necrotic lesions.

Fungal isolation

Fungal isolates were obtained from the diseased samples (leaf, neck and finger) following the protocol outlined by Longya et al. (2020) with modifications. Briefly, ~ 1 cm^2 segments of the symptomatic leaf, neck and finger were rinsed with tap water to eliminate surface contaminants and sterilized in 2% sodium hypochlorite for 1 min followed by three consecutive washes in sterile distilled water to remove excess sodium hypochlorite. The samples were air dried on sterile blotting paper (Whatman no. 1) in the laminar flow then cultured on cooled pre-autoclaved half strength potato dextrose agar (PDA) for five days. Single growing mycelium were transferred to full strength PDA medium and incubated under 24 h of constant fluorescent light at 25 ± 2°C for 14 days in the growth chamber. To induce sporulation, the mycelium was transferred onto oatmeal agar (OMA) media and incubated under constant fluorescent light at 25 ± 2°C for 14 days. To obtain monoconidia, 14-day old cultures were flooded with autoclaved distilled water. Using a dropper, a drop of the resulting solution was cultured on OMA for 24 h. With the aid of a Leica microscope (LaboMed, Beijing, China), a single growing spore was carefully transferred to a fresh OMA and PDA medium and allowed to grow for another 14 days. The resultant pure cultures were used for morphological and molecular characterization while others were stored in 50% glycerol at -20 °C for future use. The culture on OMA was used to prepare spore suspension for pathogenicity tests.

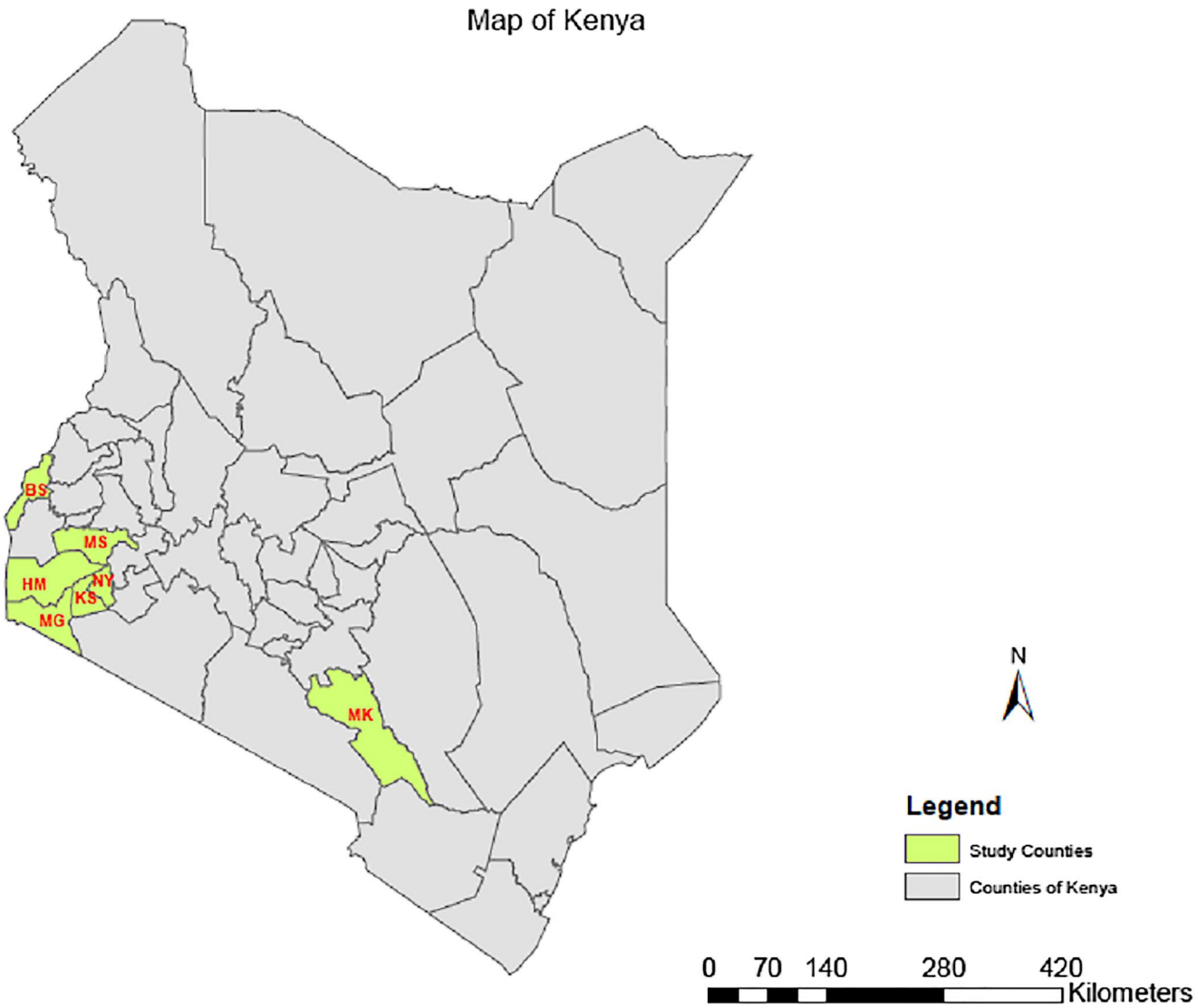


Fig. 1 A map of Kenya showing counties from which fungal isolates were collected. The codes represent Nyamira County – NY, Busia - BS, Migori – MG, Kisii – KS, Maseno in Kisumu County – MS, Homa Bay – HM and Makueni - MK

Morpho-cultural characterization

Pure isolates of monoconidial cultures grown on PDA at a temperature of 25 ± 2 °C were used for characterization. The colony characteristics such as mycelium morphology (fluffy, dense fluffy, or flat), top plate color, reverse plate color and type of margin (smooth or irregular) were recorded (Supplementary Table S2). Conidiospores were harvested by flooding pure cultures with sterile distilled water and then scrapped from the surface of the fungal mycelium with a sterile spreader. Microscopic features such as shape, colour and size (length, width and diameter) of the conidiospores were observed after staining with lactophenol cotton blue. The colony morphology (flat, fluffy, dense fluffy) and size of the conidia were measured under a Leica microscope (LaboMed, Beijing, China) using ocular and stage micrometers as described by Meena (2005). Each variable scored for colony and conidiosphore characteristics was converted into binary format where (1) denoted presence of the specific variable (for example fluffy morphology) and (0) denoted absence of the same variable (in this case, not fluffy) and used to construct a dendrogram. The dendrogram was constructed in R software (version 4.2.1) where the distance matrix and hierarchical clustering were performed using Euclidean and Ward D methods, respectively. The classification of the fungal isolates was based on the observed mycelium morphology, color and margin, conidiospore size and shape.

Genomic DNA extraction, polymerase chain reaction (PCR) and sequencing

Briefly, the stock of purified fungal isolates initially stored in 50% glycerol were transferred to petri dishes with OMA medium and incubated at 25 ± 2 °C for 7 days. Five plugs were then collected for each isolate and placed in potato dextrose broth (PDB), incubated under constant fluorescent light at 25 ± 2 °C and shaken at 130 rpm for 5 days. Mycelia of each fungal isolate were then filtered, weighed, frozen in liquid nitrogen and then stored at -80 °C prior to genomic DNA extraction. Extraction of genomic DNA from the mycelia of the fungal isolates was done by the column-based method using ISOLATE II Plant DNA Kit (Bioline Meridian Biosciences, USA) following the manufacturer's instructions. PCR amplification was carried out using fungal DNA-specific and species-specific primers for identification of *M. oryzae*. The fungal specific gene assay was carried out using *ITS5/4* primers [*ITS5* (5'GGAAGTAAA AGTCGTAACAAGG-3') and *ITS4* (5'-TCCTCCGCTTAT TGATATGC-3')], while the species-specific primers were *POT2a* [*POT2a-L2* (5'-GCAATTTCATGCAACCGAAA -3') and *Pot2a-R2* (5'-CGTACGCCAACCAGATTGAA -3')] and *Pfh2* [*Pfh2*-F (5'-CGTCACACGTTCTTCAACC -3') and *Pfh2-R* (5'-CGTTTCACGCTTCTCCG-3')]. PCR amplifications for *ITS5/4*, *Pfh2* and *Pot2a* were performed in a 20 µl volume according to the methods described by Harmon et al. (2003), Longya et al. (2020) and Pieck et al. (2017), respectively. The PCR reaction was performed in a thermocycler (GeneAmp® PCR system 9700, Applied Biosystems, Singapore) with GoTaq® Green master mix (Promega, Madison, USA). The thermal cycling conditions for *ITS5/4* primers were: initial denaturation at 94 °C for 5 min followed by 35 cycles of denaturation, annealing and extension at 94 °C for 30 s; 55 °C for 30 s, 72 °C for 1 min and a final extension at 72 °C for 5 min. The thermal cycling conditions for *Pfh2* pair were: initial denaturation at 94 °C for 90s followed by 35 cycles of denaturation, annealing and extension at 94 °C for 45 s; 55 °C for 45 s, 72 °C for 45 s and a final extension at 72 °C for 10 min. For *Pot2a* primer, the thermal cycling conditions were: initial denaturation at 94 °C for 90s followed by 35 cycles of denaturation, annealing and extension at 94 °C for 30 s; 62 °C for 30 s, 72 °C for 60 s respectively and a final extension at 72 °C for 2 min.

Sequencing, sequence analysis and genetic diversity tree construction

The amplicons were purified using EXO-CIP clean up kit (New England BIOLABS, UK) and sequenced using Sanger sequencing technique (Eurofins Genomics India Pvt Ltd., India). All *ITS5/4* amplicons were forward- and reverse-sequenced alongside one amplicon of either *Pot2a* or *Pfh2* for each of the samples, where available. The resulting forward and reverse sequences of each fungal isolate were edited using BioEdit sequence alignment editor (version 7.2.5.0) and consensus sequences created per sample per amplicon (Hall 1999). The consensus sequences were used as query against the Basic Local Alignment Search Tool (BLASTn) tool (Altschul et al. 1990) in NCBI to retrieve homologous sequences from the GenBank database. Sequences with 96–100% homology were retrieved and used in confirmation of species as well as the construction of genetic diversity tree in Molecular Evolutionary Genetic Analysis (MEGA) version X (Kumar et al. 2018). Publicly available sequences of wheat blast pathogen isolated from Zimbabwe were retrieved from public databases and used as an outgroup for each of the amplicon category. Bootstrap replications (500) were used to evaluate the statistical viability of the phylogeny while maximum likelihood method analyses was used to generate a tree in MEGA.

Pathogenicity test

Morphological and molecular data was used alongside tissue source and sampling location to select two *M. oryzae* pathotypes from different groups for pathogenicity tests. Eighteen diverse finger millet breeding lines were selected as differential set based on their morphological (Table 1) as well as genetic relatedness across a broader collection of East African breeding lines (Supplementary Fig. 1). Pathogenicity test was done in three replicates for each genotype by selecting randomly three plants per replicate and inoculating three random leaves from each selected plant. The typical severity score for blast disease is as represented in Fig. 2. The genotypes were classified as resistant (R) if the average severity ranking was 1–3.0, moderately resistant (MR) if the rating was 3.1–5.0, susceptible (S) if the ranking was 5.1–7.0 and highly susceptible (HS) if the ranking was 7.1–9.0 (Fig. 2).

The genetic clustering of 15 out of the 18 proposed differential set that was previously done based on existing Diversity Arrays Technology sequencing (DArT-seq; Sansaloni et al. 2011) data (unpublished). Non-symptomatic leaves were obtained from 14-day old plantlets of the differential set that had been grown in the polyhouse at the World Agroforestry Centre (WAC, Nairobi, Kenya). The leaves were washed with distilled water and then sterilized in 1% sodium hypochlorite for one min followed by rinsing with sterile distilled water. The leaves were then air-dried under the laminar flow on sterile paper towels. Upon drying, the leaves from each accession were placed in 90-mm diameter Petri-dishes containing moisturized blotting paper towels to maintain high moisture. The leaves were pin-pricked three times on the

Table 1 Finger millet genotypes selected for pathogenicity tests and their known field reaction to blast disease

Accession	Attributes	Genotyped	Blast reaction in the field [z]
1. IE3973	Traditional cultivar/Landrace	Yes	MR
2. ICFV18242	Improved variety, high yielding	No	S
3. KNE741	Low yielding, commercial variety	Yes	S
4. IE2187	Traditional cultivar/Landrace	Yes	S
5. ICFV182512	Improved variety, high yielding, late maturing	No	R
6. Ikhulule	Resistant to blast, Striga and lodging; drought tolerant; dark brown grain color; high yielding, commercial variety	Yes	R
7. Okhale-1	Tolerant to Striga and blast; good malting quality; lodging resistant; brown grain color; high yielding, commercial	Yes	R
8. KNE628	Improved variety, advanced breeding line, commercial variety	Yes	MR
9. IE5812	Traditional cultivar/Landrace	Yes	MR
10. IE546	Traditional cultivar/Landrace	Yes	MR
11. IE6321	Traditional cultivar/Landrace	Yes	R
12. MS18	Landrace	Yes	S
13. IE501	Traditional cultivar/Landrace	Yes	MR
14. TZ1636	Breeding line	Yes	R
15. Ekama white	High yielding, good malting quality; tolerant to blast; brown colored grains preferred by farmers; easy to thresh; lodging resistant	Yes	R
16. IE593	Traditional cultivar/Landrace	Yes	S
17. IE2008	Traditional cultivar/Landrace	Yes	MR
18. IE5635	Traditional cultivar/Landrace	Yes	MR

[z]This reaction is based on field observations recorded as MR = Moderately resistant, R = Resistant, S = Susceptible

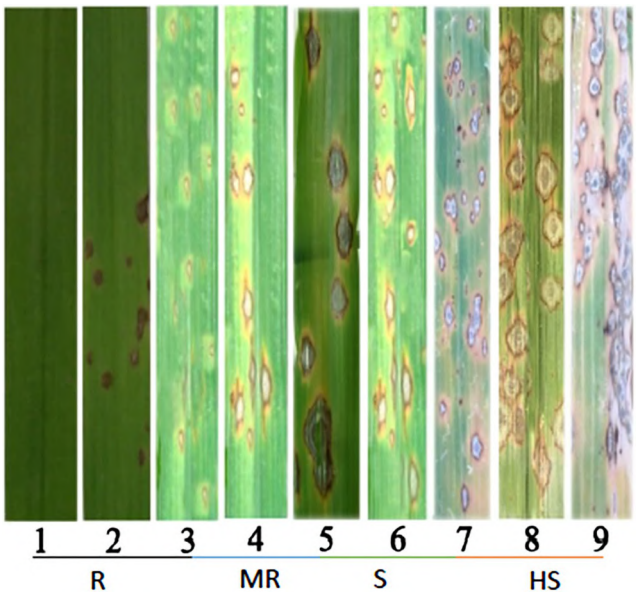


Fig. 2 Finger millet disease rating score for seedlings infected with *M. oryzae*. The 9-class disease rating scale is generally classified into four categories of resistant (R) (1.0–3.0), Moderately Resistant (MR) (3.1 -5.0), Susceptible (S) (5.1 -7.0) and Highly Susceptible (HS) (7.1 -9.0). Source: Babu et al. (2013)

upper side with a sharp sterile needle and each spot inoculated with a 5 µl drop of 1×10^5 conidia/mL concentration of spore suspension prepared from each isolate and incubated for 4 days at 25 ± 2 °C. Healthy leaves were used as control and were inoculated with sterile distilled water. After 4 days of incubation, the response of each accession was recorded in terms of the number of successfully developed lesions per leaf in a petri dish, size of lesions and severity score. The severity score was determined using a scale of 1–9 (Fig. 2; Babu et al. 2013). The experimental design was a randomized complete block design with three replicates for each fungal isolate and one leaf with three inoculation point was used per replicate. The data obtained met the assumption of normality and homogeneity while R statistical software version 4.4.2 was used to analyse the ANOVA. To complete the Koch's postulates, the fungal pathogen was re-isolated from the infected leaves and morphological characteristics were compared with the original cultures.

Results

Fungal isolation and morphological characterization

Out of the 450 samples collected that consisted of 150 each of neck, finger and leaf samples, 92 (~21%) could be

Table 2 Memberships of pure pyriform fungal isolates into different clusters and the corresponding morphological features

Cluster	Isolate ID[z]	Mycelium morphology	Top plate color	Reverse plate color	Margin	Spore diameter (µm)	Spore length (µm)	Spore shape
1A	S25, S36, S89, S88, S87, S78, S77, S73, S72, S71, S67, S63, S61, S59, S4, S22, S1, S38	Flat, fluffy	Grey: whitish grey; black	Blackish grey with white ring towards the margin	Smooth	4.0–7.0	13.0-15.9	Pyriform
1B	S66, S65, S62, S60, S42, S16, S6, S15, S44, S53, S35, S24, S19, S20, S39, S74, S64, S56, S32, S23, S30, S29, S5, S90, S2, S3	Fluffy	Whitish grey	Blackish grey with white ring towards the margin	Smooth	< 4.0–7.0	9.0–19.0	Pyriform
2B	S70, S76, S69, S68, S27, S40	Fluffy	Brown to grey	Brown	Irregular/smooth	< 4.0;	15.9–19.0	pyriform

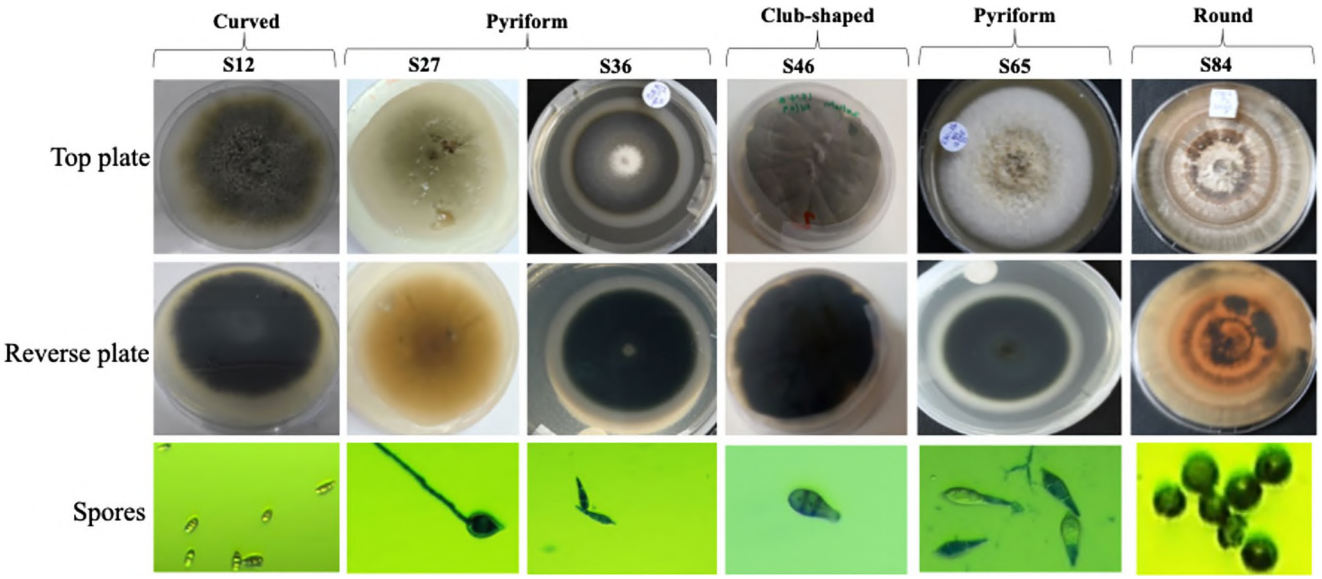


Fig. 3 Variation in morphology (mycelia and conidia) of pathogen isolates recovered from finger millet samples S12, S27, S36, S46, S65 and S84. The plate images were taken from a 14-day old cultures. The top plate spore shapes/conidia structure under light microscope at × 400 magnification are: curved, pyriform, pyriform, club-shaped, pyriform and round for isolates S12, S27, S36, S46, S65 and S84, respectively with a scale bar of 20 µm

isolated as pure fungal cultures for downstream analysis (Supplementary Table S2). Two variants (S48a and S58a) were additionally cultured from isolates S48_F and S58_L based on slight colour variations observed in plate cultures. The 94 pure cultures consisted of 48 from neck, 35 from finger and 11 from leaf tissues, indicating the difficulties in recovering pure cultures of blast disease from diseased plant tissues overall, but especially from leaf. The 94 recovered pure cultures originated from Busia (28), Kisumu (22), Kisii (18), Nyamira (12), Migori (9), Makueni (3) and Homabay (2) counties (Fig. 1). A dendrogram based on morphological characteristics identified two major clades with four sub-clusters (1A, 1B, 2A and 2B) (Supplementary Fig. 2). Based on morphological features, most of the samples within each cluster 1A, 1B, 2A, 2B were indistinguishable, revealing 5, 7, 20 and 4 distinct isolates respectively, making cluster 2A the most diverse morphologically (Supplementary Fig. 2). The fungal isolates showed considerable variations in morphological traits such as colony morphology, colony top plate and reverse plate color as well as conidial shape, length and diameter (Table 2; Supplementary Table S2; Fig. 3, Supplementary Fig. 2). Colony margins were either smooth or irregular/rough with colors ranging from white, grey black, black, brown and maroon (Table 2; Fig. 3). The isolates which produced pyriform conidia; a typical feature of *Pyriculariaceae*, were found in cluster 1A,1B and 2B forming the first basis of *M.oryzae* identification (Table 2; Fig. 3).

Molecular identification of the fungal isolates using *ITS5/4*

All the 92 pure cultures and one variant (S48a) of fungal isolates could be amplified using *ITS5/4* primer set resulting in amplicons of ~567 bp after aligning forward and reverse sequences of each isolate. Four amplicons (S4_N, S20_L and S55_N and S91_N) generated poor quality sequences and were therefore dropped from further analysis. A consensus sequence of the remaining 89 isolates was used to retrieve 62 other highly similar (at least 96%) sequences from NCBI that were representative of *Magnaporthe* spp. and closely related species. Diversity analysis of the 151 sequences clustered 47 of the 89 *ITS5/4*-amplified isolates with other *Magnaporthe* spp., 27 clustered with *Epicoccum* spp., 6 clustered with *Curvularia* spp., 4 with *Alternaria* spp., 3 with *Nigrospora* spp. and 2 with *Arthrinium* spp. (Fig. 4). *M. oryzae* clade was further separated into 3 distinct sub-clusters; one of predominantly *M. oryzae Eleusine* (*MoE*) isolates, a second one having both *M. oryzae Setaria* (*MoS*) and *M. oryzae Oryzae (MoO)* isolates, and a third one of predominantly *M. oryzae Triticum* (*MoT*) isolates (Fig. 4). All the 47 amplified finger millet isolates were distinctly clustered as *MoE* except one (S65_F) that was different from all the *Magnaporthe* spp. The *M. grisea* clade revealed two sub-clusters, one with 7 pearl millet isolates and another of 3 *Digitaria* spp. isolates (Fig. 4).

Of the 46 *ITS5/4* amplicons correctly identified as *MoE,* one was from a leaf sample, 16 from finger and 29 from neck isolates (Fig. 4). In comparison to the morphological clustering, seventeen (S73_N, S78_F, S1_N, S36_N, S71_N, S63_N, S72_F, S67_F, S77_N, S25_F, S89_F, S61_N, S88_F, S38_N, S59_N, S22_F, S87_N) out of 18 isolates that were grouped under 1A using morphological features were correctly identified using *ITS5/4* markers (Figs. 3 and 4). Twenty-three out of 26 isolates that grouped under morphological cluster 1B were correctly identified using *ITS5/4* markers except for S65_N, S20_L, S74_F, S29_L. Half of the isolates that were grouped under morphological cluster 2B were correctly identified as *MoE* using *ITS5/4* markers – these were S27_N, S70_N, S40_F, S68_N, S69_F, S76_F (Fig. 4). No specific clustering based on tissue type was observed.

Molecular identification of the fungal isolates using *Pfh2*

Pfh2 amplification produced a single band of ~687 bp from 59 pure culture isolates, of which 30 pure culture amplicons and one variant (S58a) were sequenced. Consensus sequences of each of the isolates were retained after aligning forward and reverse sequences. The 30 consensus sequences consisted of 16 isolates that had been previously correctly clustered under the *MoE* cluster using *ITS5/4* primers (Fig. 4), as well as 12 isolates that were clustered with other fungal species using *ITS5/4*, and one additional isolate (S55_N) that was not included in the *ITS5/4* analysis due to poor sequence quality. A consensus sequence of the 30 isolates was used to retrieve 52 other highly similar (at least 96%) sequences from NCBI that were representative of *Magnaporthe* spp. although the sequences that were publicly available were mainly from rice and finger millet isolates. Genetic diversity analysis of the 82 sequences revealed two major clusters, one cluster of the 30 finger millet amplicons alongside one other publicly available finger millet isolate, and a second cluster comprising of publicly available sequences from rice isolates (Fig. 5).Twelve out of the 30 isolates did not previously cluster with *Magnaporthe* spp. using *ITS5/4* primers suggesting that *Pfh2* may not be a precise primer set for accurately distinguishing *Magnaporthe* spp. from other closely related species. Overall, *Pfh2* validated 16 (S78_F, S56_F, S23_N, S30_N, S90_N, S29_L, S77_N, S25_F, S53_F, S89_F, S16_N, S24_N, S15_F, S76_F, S22_F, S19_N) isolates out of the 46 already identified using *ITS5/4* primers but could not further distinguish them from other closely related species, perhaps due to lack of sequences from other non-*Magnaporthe* spp. from the public databases (Fig. 5).

Molecular identification of the fungal isolates using *Pot2a*

Pot2a amplification produced a single band of 389 bp from 47 isolates, of which 30 amplicons were sequenced and used for further genetic diversity analysis. Twenty-six additional highly similar (at least 96%) sequences were retrieved from NCBI from diverse hosts. Genetic diversity analysis of the 56 sequences revealed two major clades, one that contained 2 sub-clusters of *Eleusine* and *Oryzae* isolates, and a smaller clade with 2 small sub-clusters of *Oryzae* and *Triticum* isolates (Fig. 6). Twenty-eight out of the 30 *Pot2a* amplicons validated isolates that had previously been identified using *ITS5/4*, one (S19_N) of which was also validated using *Pfh2* primers (Supplementary Fig. 6). One more isolate (S65_F) that out-grouped the *ITS5/4 MoE* cluster, perhaps due to poor sequence quality, was further confirmed as *MoE* using *Pot2a* (Figs. 4 and 6). One isolate, S20_L that could not be analysed using *ITS5/4* due to poor sequence quality was amplified by *Pot2a* and correctly clustered with other *MoE* isolates (Fig. 6).

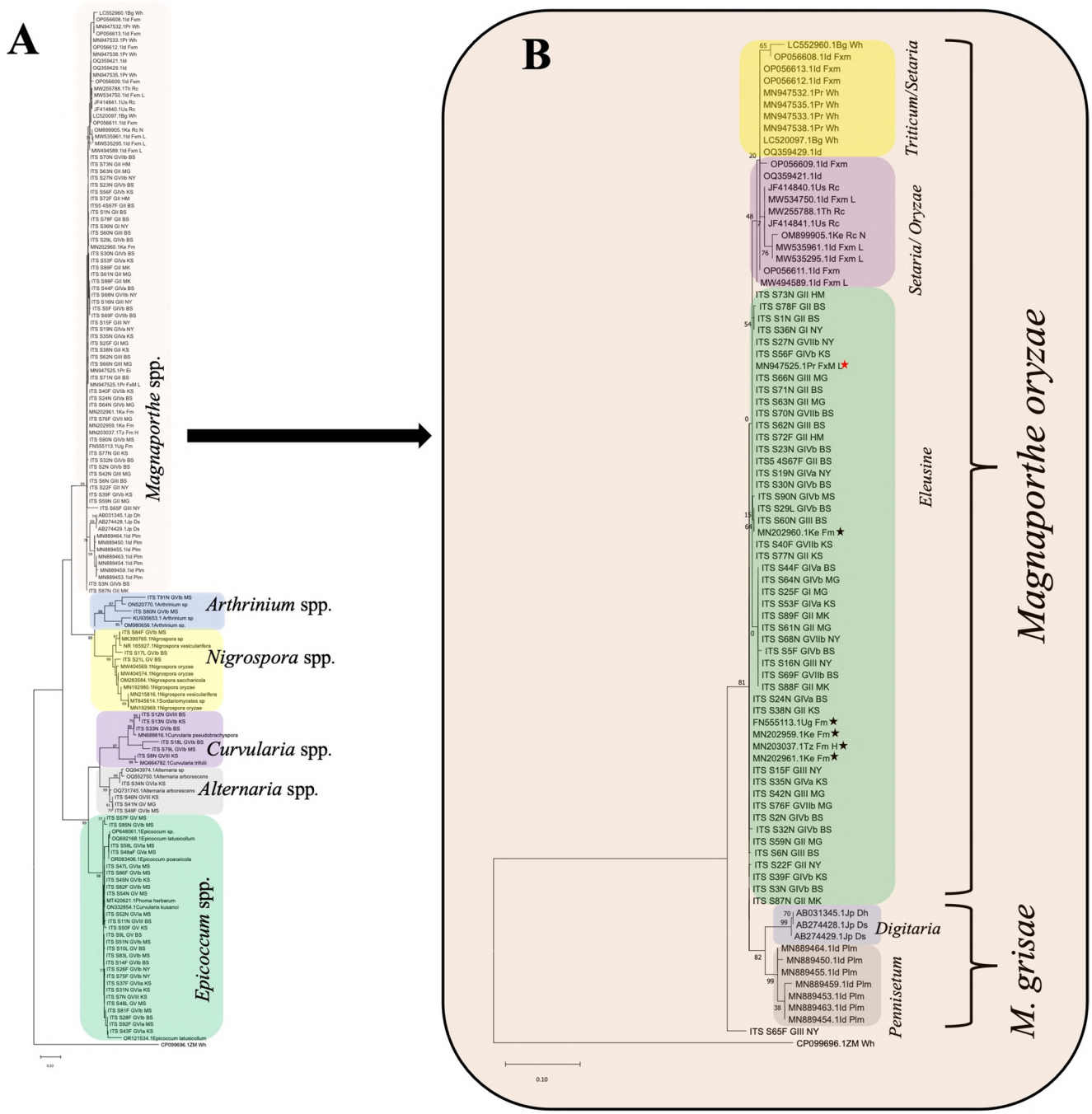


Fig. 4 Genetic diversity trees constructed by MEGA X based on internal transcribed spacer (*ITS5/4*) sequences. It shows the clustering of *Magnaporthe* spp. clearly distinguishing *M. grisea* from *M. oryzae*. The isolates clustered by host except the red star pointing at foxtail millet isolate clustering with *Eleusine* isolates. Black stars highlight other *Eleusine* isolates from public databases. KEY. The country of origin of isolates used as reference sequences from the GenBank database are represented as: Us = USA, Ke = Kenya, Id = India, Tz = Tanzania, Tw = Taiwan, Ug = Uganda, Pr = Paraguay, Jp = Japan, Th = Thailand, Bg = Bangladesh, ZM =– Zimbabwe. The different hosts from where the isolates used as reference sequences are represented as: Fxm = foxtail millet, Wh = Wheat, Fm = Finger millet, Rc = Rice, Ds & Dh = crab grass, Plm = Pearl millet, Ei = *Eleusine indica*. For the sequences in this study and those obtained from the GenBank, the plant tissue where the isolate was collected are represented as L = leaf, N = neck, F = Finger, S = seed

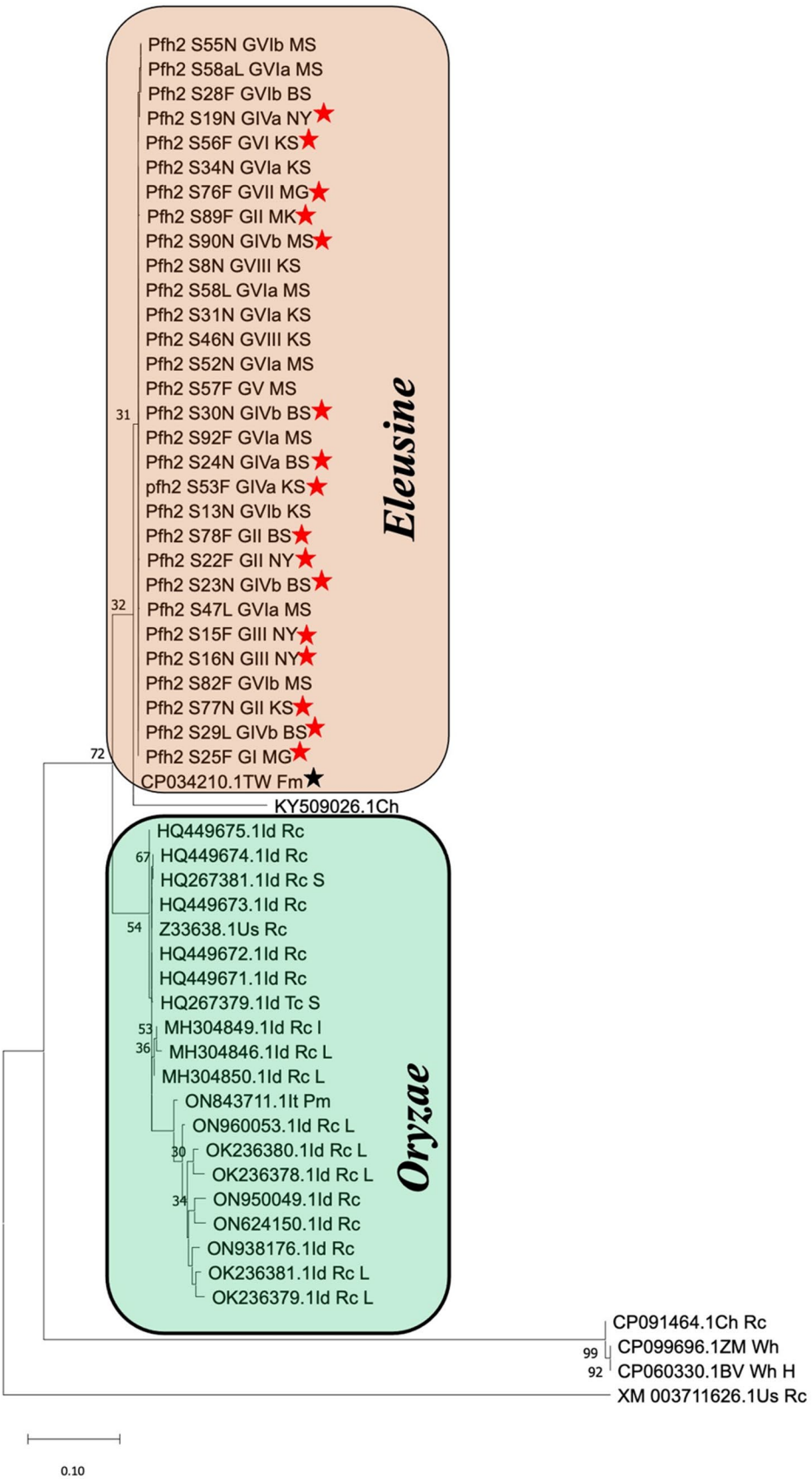


Fig. 5 Genetic diversity tree constructed based on multiple sequence alignment of *Pfh2* nucleotide sequences. The tree was generated using maximum likelihood method with 500 bootstrap replications in MEGA X. Black stars highlight other *Eleusine* isolates from public databases while red stars highlight isolates that were previously correctly identified as *Eleusine* using *ITS5/4* primers. The country of origin of isolates used as reference sequences from the GenBank database are represented as: Us = USA, Id = India, Tw =Taiwan, BV=Bolivia, ZM = Zimbabwe. The different hosts from where the isolates used as reference sequences are represented as: Pm - Proso millet, Wh = Wheat, Fm = Finger millet and Rc = Rice. For publicly retrieved sequences, where information was available on the tissue from which the isolate was collected, we added letters L, N, F, H and S at the end of each isolate name to represent leaf, neck, finger, head and seed respectively

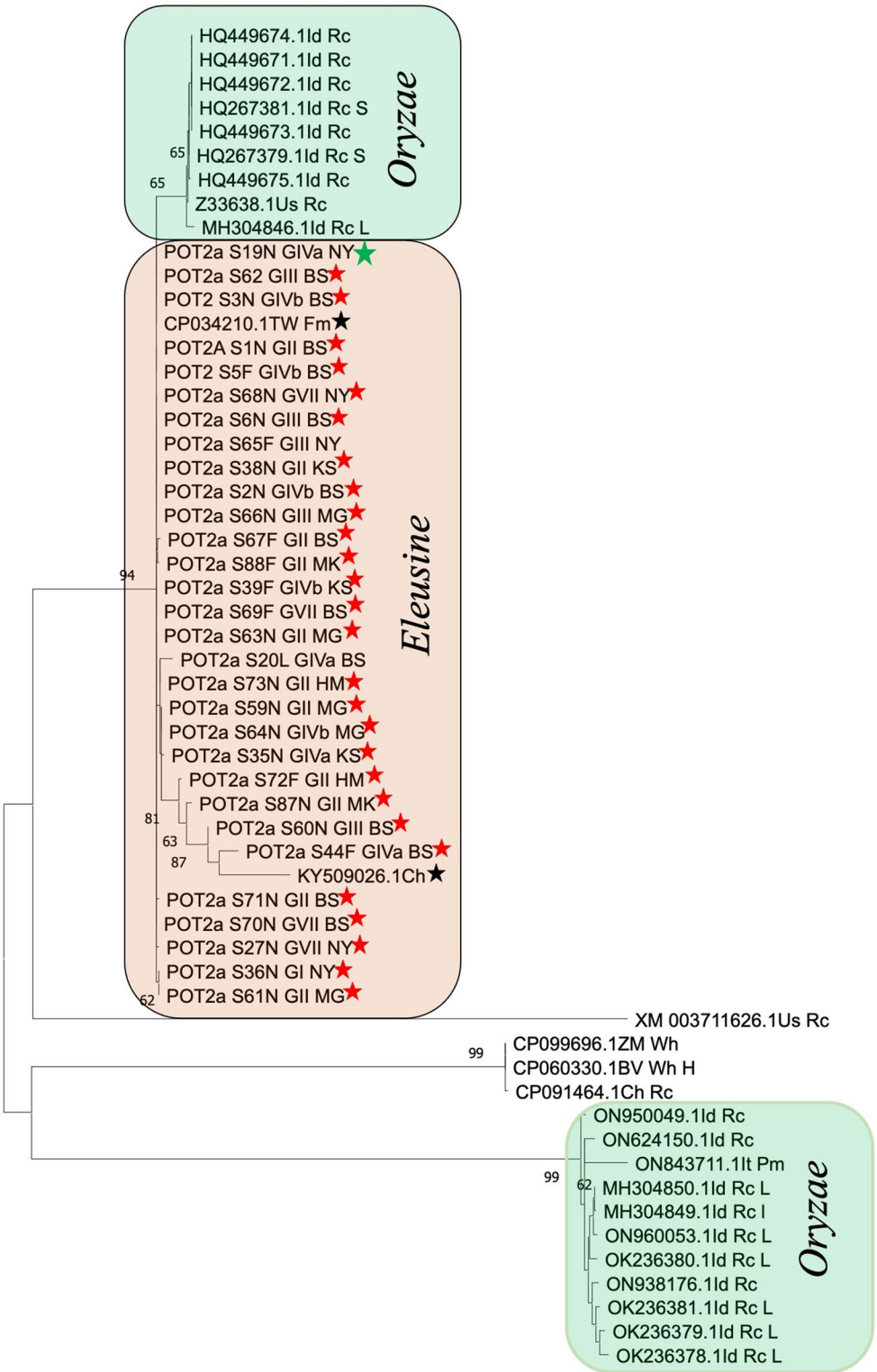


Fig. 6 Phylogenic tree constructed based on multiple sequence alignment of *Pot2a* nucleotide sequences of *M. oryzae* isolates. The tree was generated using maximum likelihood method with 500 bootstrap replications in MEGA X. Black stars highlight other *MoE* isolates from public databases while red stars highlight isolates that were already correctly identified as *Eleusine* using *ITS5/4*. Green star highlights the isolate that was correctly identified using all the three primers. The country of origin of isolates retrieved from public databases are represented as: Us - USA, Id = India, Ch= China, BV = Bolivia, Tw = Taiwan, ZM = Zimbabwe. The different hosts from where the publicly available isolates were collected from are represented as: Pm = Proso millet, Wh = Wheat, Fm = Finger millet and Rc = Rice. For the sequences generated from this study, the plant tissue where the isolate was collected is represented as L = leaf, N = neck, F = Finger. S at the end of publicly retrieved sequences denotes "Seed" as the tissue from which isolate was detected

Genetic diversity analysis of the Kenyan *MoE* isolates

The total number of finger millet blast isolates that were correctly identified using at least two markers was 44 (Table 3). They were all pyriform with spore length ranging from 9.3 to 19 µm and spore diameter ranging 2.1–6.3 µm (Table 3). The correctly identified isolates were all from morphological cluster 1, except 5 (S27_N, S68_N, S69_F, S70_N, S76_F) that were from morphological cluster 2B

Table 3 A list of blast isolates that were correctly identified as true *Eleusine* based on at least one of the primer pairs

Isolate Name/Tissue/Region	Morphological cluster	Spore diameter (µm)	Spore length (µm)	Spore shape	ITS5/4 (amplicon) sequenced	Pfh2 (amplicon) sequenced	Pot2a (amplicon) Sequenced
1. S1_N_BS	1A	5.1	13.9	Pyriform	YES	NO	YES
2. S2_N_BS	1B	3.3	16.4	Pyriform	YES	NO	YES
3. S3_N_BS	1B	2.9	17.8	Pyriform	YES	NO	YES
4. S5_F_BS	1B	3.8	18.0	Pyriform	YES	NO	YES
5. S6_N_BS	1B	3.3	12.8	Pyriform	YES	NO	YES
6. S15_F_NY	1B	2.8	11.5	Pyriform	YES	YES	NO
7. S16_N_NY	1B	3.8	11.8	Pyriform	YES	YES	NO
8. S19_N_NY	1B	5.2	15.8	Pyriform	YES	YES	YES
9. S22_F_NY	1A	5.1	14.2	Pyriform	YES	YES	NO
10. S23_N_BS	1B	3.9	17.2	Pyriform	YES	YES	NO
11. S24_N_BS	1B	4.9	13.5	Pyriform	YES	YES	NO
12. S25_F_MG	1A	5.0	14.5	Pyriform	YES	YES	NO
13. S27_N_NY	2B	3.1	17.0	Pyriform	YES	NO	YES
14. S29_L_BS	1B	3.5	16.6	Pyriform	YES	YES	NO
15. S30_N_BS	1B	2.8	18.8	Pyriform	YES	YES	NO
16. S35_N_KS	1B	6.3	15.7	Pyriform	YES	NO	YES
17. S36_N_NY	1A	4.3	13.8	Pyriform	YES	NO	YES
18. S38_N_KS	1A	4.5	14.6	Pyriform	YES	NO	YES
19. S39_F_KS	1B	3.1	17.4	Pyriform	YES	NO	YES
20. S44_F_BS	1B	5.3	15.4	Pyriform	YES	NO	YES
21. S53_F_KS	1B	4.3	14.8	Pyriform	YES	YES	NO
22. S56_F_KS	1B	2.9	16.4	Pyriform	YES	YES	NO
23. S59_N_MG	1A	4.6	13.0	Pyriform	YES	NO	YES
24. S60_N_BS	1B	3.6	12.8	Pyriform	YES	NO	YES
25. S61_N_MG	1A	5.3	14.8	Pyriform	YES	NO	YES
26. S62_N_BS	1B	2.6	11.6	Pyriform	YES	NO	YES
27. S63_N_MG	1A	6.3	15.8	Pyriform	YES	NO	YES
28. S64_N_MG	1B	2.4	18.8	Pyriform	YES	NO	YES
29. S65_F_NY	1B	2.3	9.3	Pyriform	YES	NO	YES
30. S66_N_MG	1B	2.1	12.3	Pyriform	YES	NO	YES
31. S67_F_BS	1A	3.7	13.8	Pyriform	YES	NO	YES
32. S68_N_NY	2B	2.2	19.0	Pyriform	YES	NO	YES
33. S69_F_BS	2B	3.9	16.4	Pyriform	YES	NO	YES
34. S70_N_BS	2B	2.9	18.0	Pyriform	YES	NO	YES
35. S71_N_BS	1A	4.0	13.6	Pyriform	YES	NO	YES
36. S72_F_HM	1A	5.0	13.6	Pyriform	YES	NO	YES
37. S73_N_HM	1A	4.4	13.2	Pyriform	YES	NO	YES
38. S76_F_MG	2B	3.8	16.0	Pyriform	YES	YES	NO
39. S77_N_KS	1A	5.7	15.8	Pyriform	YES	YES	NO
40. S78_F_BS	1A	5.5	14.2	Pyriform	YES	YES	NO
41. S87_N _MK	1A	5.0	14.4	Pyriform	YES	NO	YES
42. S88_F_MK	1A	5.0	14.3	Pyriform	YES	YES	NO
43. S89_F_MK	1A	6.3	15.2	Pyriform	YES	YES	NO
44. S90_N_MS	1B	2.1	17.0	Pyriform	YES	YES	NO

(Supplementary Fig. 2). Further genetic diversity analysis of the confirmed *MoE* isolates based on *ITS5/4* and *Pot2a* sequences revealed some level of differentiation of isolates (Fig. 7). *ITS5/4* revealed three major clusters with cluster I comprising of 27 isolates with likely 3 variants (one from Kisumu and two from Busia); cluster II contained 15 isolates, four of which differentiated into a sub-cluster, while cluster III comprised of nine isolates, four of which were retrieved from public databases (Fig. 7A). *Pot2a* grouped the isolates into one major cluster with potentially four sub-clusters of variants (Fig. 7B). *Pfh2* could not adequately distinguish the various isolates (Fig. 7C).

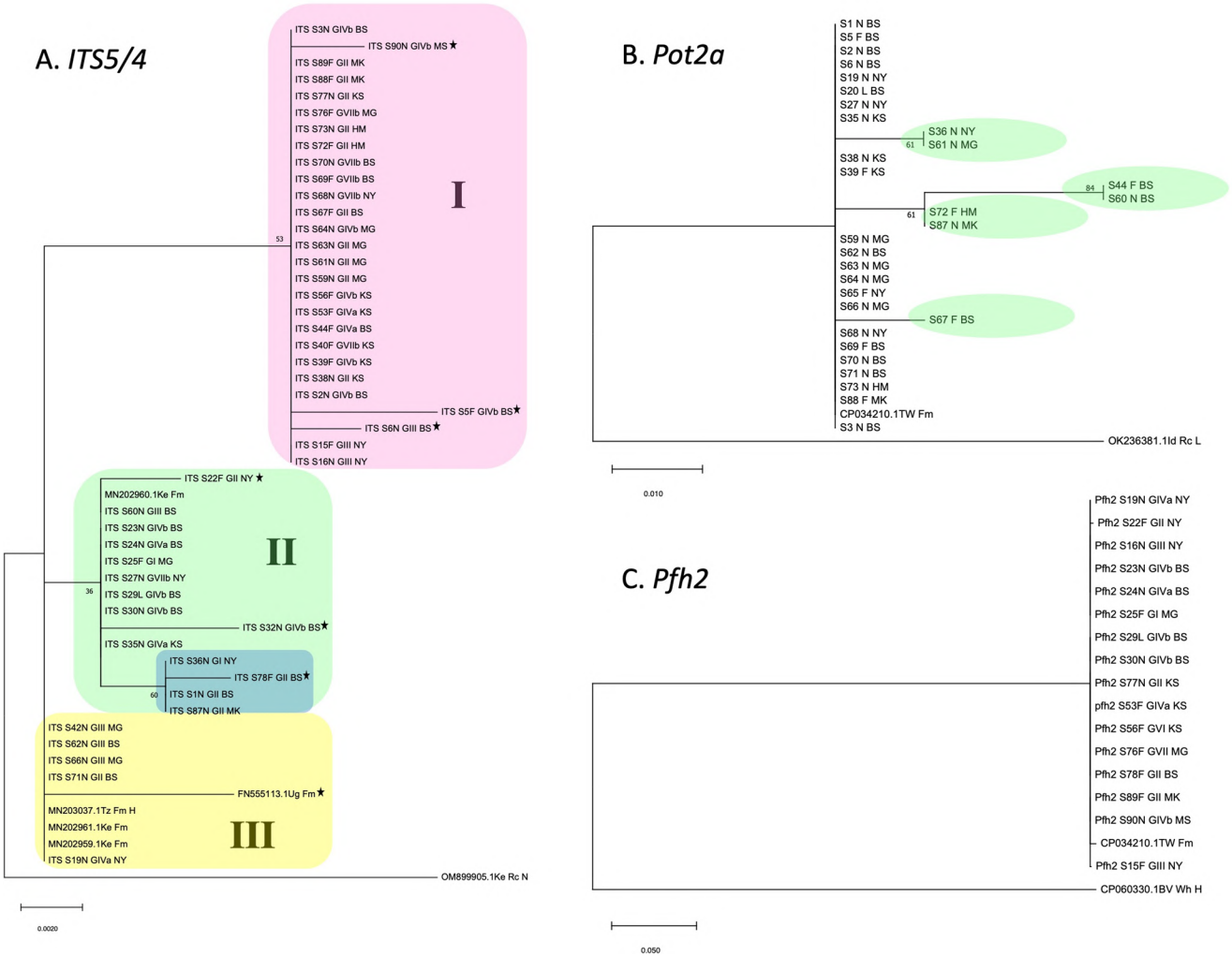


Fig. 7 Genetic diversity trees of confirmed *MoE* isolates constructed by MEGA X based on the amplicons of the 3 genes and rooted with either *MoO* or *MoT* isolates that had been retrieved from public databases. All trees were generated using maximum likelihood method with 500 bootstraps. (**A**) *ITS5/4* tree rooted using *MoO* isolate OM899905.1Ke_Rc_N. Isolates with black stars appear as variants from the same cluster. The 3 major clusters are labeled while a sub-cluster is highlighted in blue color under cluster II. (**B**) *Pot2a* tree rooted using *MoO* isolate OK236381.1ld_Rc_L. Potential variants are highlighted in green circles. (**C**) *Pfh2* tree rooted using *MoT* isolate CP060330.1BV_Wh_H

Pathogenicity tests

The two randomly selected isolates, S2_N_BS and S72_F_HM from Busia and Homa Bay counties respectively exhibited varying levels of pathogenicity across the 18 host differentials (Table 4). The typical symptom observed on the leaves of sensitive finger millet accessions were similar to the symptoms observed in the field (Fig. 2). Significant ($P < 0.001$) differences were observed for the number of lesions, lesion size and blast severity score for the 18 host differentials evaluated (Table 5). Infections with both isolates resulted in observed symptoms across all the 18 host differentials (Table 4). Based on a scale of 1– 9 (Fig. 2; Babu et al. 2013). The genotypes were classified as resistant (R) if the average severity ranking was 1–3.0, moderately resistant (MR) if the rating was 3.1–5.0, susceptible (S) if the ranking was 5.1–7.0 and highly susceptible (HS) if the ranking was 7.1–9.0 (Table 4). Five genotypes (IE3973, IE5812, IE546, IE6321, IE5635) revealed a consistent R response between both isolates, three genotypes (OKHALE-1, IE501, IE2008) were consistently MR while 2 genotypes (ICFV182427 KNE741 and MS18 IE2187) were consistently S across S2_N_BS and S72_F_HM isolates (Table 4). Two genotypes (ICFV182427 and IE2187) were HS in one and S in the other isolate. Other than ICFV182512 that was S against S2_N_BS but R against S72_F_HM, all the remaining genotypes were either S/R to one isolate and MR to the other (Table 4). Our results confirmed the co-existence of other fungal pathogens on the same tissues with *MoE*, and revealed the distinctness of two randomly selected blast isolates in their ability to cause disease across different finger millet genotypes.

Table 4 Disease response of finger millet host differentials following inoculation with two *Magnaporthe oryzae* isolates (S2 and S27) under in vitro conditions

Finger millet accession	S2_N_BS				S72_F_HM			
	No. of Lesions	Length of Lesions	Blast severity score (1–9)[y]	Reaction[z]	No. of Lesions	Length of Lesions	Blast severity score (1–9)[y]	Reaction[z]
1. IE3973	0.67 ± 0.58	2.27 ± 1.98^{efg}	2.33 ± 0.58^{fg}	R	1 ± 0.00^{bcd}	1.99 ± 0.67^{efg}	3 ± 0.00^{cdef}	R
2. ICFV182427	2.67 ± 0.58^{ab}	7.86 ± 0.98^{bcde}	8.33 ± 0.58^{ab}	HS*	1.33 ± 0.58^{abcd}	7.49 ± 0.77^{bcd}	6.33 ± 0.58^{ab}	S*
3. KNE741	2.33 ± 0.58^{abc}	11.76 ± 1.01^{ab}	6.33 ± 0.58^{abcd}	S	2.33 ± 0.58^{a}	9.65 ± 0.78^{abc}	6.33 ± 0.58^{ab}	S
4. IE2187	2 ± 0.0^{abc}	14.20 ± 0.28^{a}	9 ± 0.0^{a}	HS*	2 ± 0.00^{ab}	11.21 ± 0.88^{ab}	6.33 ± 0.58^{cdef}	S*
5. ICFV182512	2.33 ± 0.58^{abc}	10.38 ± 0.25^{abc}	7 ± 0.00^{abc}	S*	1.67 ± 0.58^{abcd}	4.32 ± 0.81^{def}	3 ± 0.0^{cdef}	R*
6. IKHULULE	1 ± 0.00^{abc}	5.78 ± 1.09^{cdefg}	3 ± 0.00^{efg}	R*	1 ± 0.00^{bcd}	5.78 ± 1.09^{cde}	4.33 ± 0.57^{abcde}	MR*
7. OKHALE-1	2.33 ± 0.58^{abc}	7.13 ± 0.71^{bcdef}	5 ± 0.00^{cdef}	MR	2 ± 0.00^{abc}	8.71 ± 0.45^{abc}	5 ± 0.00^{abcd}	MR
8. KNE628	1.33 ± 0.58^{abc}	8.13 ± 0.71^{bcd}	4.33 ± 0.58^{cdefg}	MR*	1.33 ± 0.58^{abcd}	4.03 ± 0.43^{def}	3 ± 0.00^{cdef}	R*
9. IE5812	1.33 ± 0.58^{abc}	6.04 ± 1.00^{bcdefg}	3 ± 0.00^{efg}	R	1 ± 0.00^{bcd}	4.17 ± 1.30^{def}	3 ± 0.00^{cdef}	R
10. IE546	0.67 ± 0.58^{bc}	3.62 ± 3.19^{defg}	2.33 ± 0.58^{fg}	R	0.67 ± 0.58^{cd}	0.17 ± 0.20^{fg}	1 ± 0.00^{f}	R
11. IE6321	0.67 ± 0.58^{bc}	1.47 ± 1.29^{fg}	2.33 ± 0.58^{fg}	R	0.67 ± 0.58^{cd}	0.59 ± 0.61^{fg}	1.67 ± 0.58^{ef}	R
12. MS18	3 ± 1.0^{a}	7.85 ± 1.00^{bcd}	7 ± 0.00^{abc}	S	1.33 ± 0.58^{abcd}	7.29 ± 0.61^{bcd}	5.67 ± 0.58^{abc}	S
13. IE501	2.33 ± 0.58^{abc}	8.08 ± 2.87^{bcd}	5.67 ± 0.58^{bcde}	MR	1 ± 0.00^{bcd}	5.92 ± 3.52^{cde}	4.33 ± 0.58^{abcde}	MR
14. TZ1636	2 ± 1.00^{abc}	4.28 ± 0.47^{defg}	3.67 ± 0.58^{defg}	MR*	1 ± 0.00^{bcd}	0.97 ± 1.68^{fg}	1.67 ± 0.58^{ef}	R*
15. Ekama white	1 ± 1.00^{abc}	2.70 ± 2.34^{defg}	3.67 ± 1.15^{defg}	MR*	0.67 ± 0.58^{cd}	1.73 ± 2.03^{fg}	2.33 ± 0.58^{def}	R*
16. IE593	1.67 ± 0.58^{abc}	11.58 ± 4.46^{ab}	7 ± 0.00^{abc}	S*	1.67 ± 0.58^{abcd}	8.79 ± 1.21^{abc}	5 ± 0.00^{abcd}	MR*
17. IE2008	2 ± 1.00^{abc}	4.34 ± 0.91^{defg}	3.67 ± 0.58^{defg}	MR	1 ± 0.00^{bcd}	4.34 ± 0.91^{def}	3.67 ± 0.58^{bcdef}	MR
18. IE5635	0.33 ± 0.58^{c}	0.85 ± 1.48^{g}	2.33 ± 0.58^{fg}	R	1 ± 0.00^{bcd}	2.71 ± 0.68^{efg}	3 ± 0.00^{cdef}	R
Control (SDW)	0^{c}	0^{g}	1 ± 0.0		0^{d}	0^{g}	1 ± 0.0^{f}	

[z]Blast disease response was rated as either R = Resistant, MR = Moderately resistant, S = Susceptible, HS = Highly susceptible. SDW = Sterile distilled water. Data are the means of three replicates

[y]Disease severity score is measured based on 1–9 scale, where 1–3 (R); 3.1–5 (MR); 5.1–7.0 (S); 7.1 -9 (HS); *highlights severity scores that were different between the two isolates

Means of separation are indicated with superscript letter codes for the parameters tested. Same letter code indicates no significant difference observed; Alpha = 0.05

Table 5 ANOVA table showing levels of variation across genotypes and their response to blast strains

Source of Variation	Df[y]	No. of Lesions[z]	Length of Lesions[z]	Blast Severity Score[z]
Genotype	17	4.491e-12***	< 2.2e-16***	< 2.2e-16***
M. oryzae strain	1	0.0017**	1.029e-05***	2.566e-06***
Genotype x *M. oryzae* strain		0.0285*	0.0042**	0.00021***

[z]The levels of significance were recorded as, ***Significant at $P < 0.001$; **Significant at $P < 0.01$; *Significant at $P < 0.05$;

[y]DF - Degrees of freedom

Discussion

The current study undertook a comprehensive morphological and molecular identification of *M. oryzae* isolates from seven finger millet growing counties in Kenya. Our results indicate the difficulty in successful culturing of symptomatic *M. oryzae* samples from symptomatic tissues with a success rate of 20% overall. This poor recovery rate has been reported in other studies (Rajashekara et al. 2016), but could also be due to the protocol used, the false identification of blast symptoms, or the masking of blast by other pathogens. Our isolation method (Longya et al. 2020) was slightly modified from a relatively simple to use protocol for isolating pure cultures of *Magnaporthe* spp. (Jia et al. 2009). Other protocols that have been used successfully include the spore-drop method (Palanna et al. 2023) and the glass pestle method (Farman et al. 2017). The isolation of *Magnaporthe* spp. fungus is reported to be a challenging task due to the natural occurrence of the pathogen with many saprophytic fungi (Prakash et al. 2016; Odeph et al. 2021). Given the increasing interest in studying *Magnaporthe* spp., a more reliable and reproducible protocol for in vitro isolation and maintenance of cultures will need to be developed.

Blast isolates from this study exhibited extensive variation in their morphological features such as colony appearance and conidia size. Despite the clear variation in the morpho-cultural characteristics of the fungal isolates, the pyriform conidia was a clear distinguishing feature for the isolates identified as *Magnaporthe* spp. Several studies involving *Magnaporthe* spp. have reported the spore shape to be pyriform irrespective of the host (Aruna et al. 2016; Longya et al. 2020; Palanna et al. 2024; Panda et al. 2017). However, there are other known pathogens that show pyriform shape in culture including *Alternaria* spp. (He et al. 2024) and *Curvularia* spp. (Farooq et al. 2023). Our study also identified several non-*Eleusine* isolates with pyriform

conidia implying conidia shape alone would be insufficient for identifying *Magnaporthe* spp. The other morphological feature analysed was spore length, which ranged from 9.3 to 19 µm. The spore length of *Magnaporthe* spp. has been reported to vary both within and across hosts (Longya et al. 2020; Palanna et al. 2024). *MoE* isolates from India reported spore length that ranged from 17.4 to 28.4 µm (Palanna et al. 2024). The spore length of *M. oryzae Oryzae* isolates has also been shown to vary depending on regions. A study of *MoO* in India reported spore length ranging from 18 to 25 µm (Vanaraj et al. 2013) while others reported 20–23 µm in Mali (Mahamadou et al. 2022).

We also observed no correlation between morphological characteristics of the isolates and the tissue type or geographical distribution, consistent with other similar studies (Palanna et al. 2024; Puri and Kumar 2012). The clustering of most non-*Eleusine* isolates (27 out of 43) with *Epicoccum* spp. was not surprising. A similar study in Kenya (Muthomi and Mutitu 2003) on wheat reported *Epicoccum* as the most predominant fungus followed by *Alternaria* spp., a pattern consistent with the current study. *Epicoccum* spp. have been associated with diseases of 46 plant species with leaf spot as the most common symptom (Taguiam et al. 2021), which makes it possible to confuse its symptom with that of blast. An alternative study characterizing fungal isolates from finger millet in Kenya also reported the identification of *Epicoccum* spp. alongside *Curvularia*, *Phoma* and *Alternaria* spp. from finger millet using *ITS* and *28 S* rDNA primers (Odeph et al. 2021). The high number of *Epicoccum* isolates will require further analysis given their likely economic importance as disease causing agents (Shi et al. 2024).

Our results provide evidence that morphological characterization alone is not sufficient to identify blast isolates as *MoE*. However, the pyriform feature could be used as an initial elimination step before proceeding for molecular analysis. Molecular analysis was therefore crucial for the robust identification of the isolates. We chose three fungal -specific and species-specific primers for molecular identification of *M. oryzae*. *ITS5/4* region has been previously used for the detection, identification, and classification of *Magnaporthe* isolates (Abed-Ashtiani et al. 2016; Hirata et al. 2007; Palanna et al. 2024) and found suitable to identify *Magnaporthe* at the species, or lower level (Abed-Ashtiani et al. 2016). *The ITS5/4* sequences of *MoE* isolates generated in the current study were clearly distinct from those previously sequenced from foxtail millet, rice and wheat. The availability of sequences from other related species for *ITS5/4* in public databases made it possible to eliminate isolates that were likely *Curvularia* spp., *Epicoccum* spp., *Phoma* spp., *Alternaria* spp., *Arthrinium* spp., and *Nigrospora* spp. However, this was not the case for amplicons generated using *Pfh2* primer due to the lack of publicly available *Pfh2* sequences for *Epicoccum* spp., *Alternaria* spp. and *Curvularia* spp. *Pot2a* primers validated true *Eleusine* isolates in combination with *ITS5/4*. This result was consistent with previous studies where *Pot2a* primers amplified isolates of *Triticum*, *Setaria*, *Eleusine* and *Lolium* spp. (Pieck et al. 2017). We therefore recommend the combination of morphological characterization with *ITS5/4* as well as *Pot2a* for true identification of *MoE* isolates.

Species-specific PCR detection tools have been adapted for rapid diagnosis of various *M. oryzae* pathotypes. For instance, *MoT* primers have been shown to be specific to wheat and *Bromus* spp. pathotypes (Pieck et al. 2017). The *Pfh2* primer has been used successfully to amplify a region of 687 bp of *Pot2* transposon in *M. oryzae* pathotypes collected from rye grass, wheat and rice (Gupta et al. 2020; Harmon et al. 2003; Terensan et al. 2022. In the current study we tested the specificity of *Pfh2* on *MoE* isolates for the first time. *Pfh2* primer amplified *MoE*, *Epicoccum* spp., *Curvularia* spp. and *Alternaria* spp. indicating that the primer is non-specific, contrary to earlier reports that it only amplifies *Magnaporthe* spp. (Gupta et al. 2020; Harmon et al. 2003). We therefore do not recommend the use of *Pfh2* primer in future studies for its lack of specificity in amplifying *M. oryzae* pathogens only and the failure to differentiate the *MoE* isolates.

The findings from all the three primer pairs alongside the morphological analysis indicate that *MoE* isolates co-exist with other fungal pathogens, six species of which could be identified. Previous studies also reported co-existence of blast disease in Kenya with C*urvularia* spp., *Epicoccum* spp. and *Alternaria* spp. (Odeph et al. 2021). It is not clear if some of the additional pathogens enhanced or masked the blast symptoms observed. *Curvularia trifolii*, one of the pathogens that clustered with an isolate collected from neck tissue in Kisii County, has been reported to cause leaf spot symptoms in turfgrasses (*Agrostis* spp.) (Coelho et al. 2020; Falloon 1976). *Curvularia eleusinicola* was recently reported as a novel species associated with cereal crops and weedy grass hosts (Ferdinandez et al. 2021). These reports suggest that further characterization of the additional fungal species identified in our study will need to be done to assess their economic relevance.

Further genetic diversity analysis of the identified *MoE* isolates was possible using *ITS5/4* and *Pot2a* sequences. The results from both gene amplicons indicated potential existence of different variants/pathotypes within Kenya, although additional analysis will be required for validation. In addition to the pathogenicity studies done in the current study, future investigations will need to strategically select representative isolates from each of the clusters generated from the *ITS5/4* and *Pot2a* analysis to confirm potential virulence differences. Obvious targets would be the isolates

appearing as variants from the *ITS5/4* clustering and those that were highlighted in green under *Pot2a* clustering. Testing these selected isolates across the current set of 18 genotypes as differentials would create a reference baseline for future blast pathotype characterization in Kenya. The two isolates (S2_N_BS and S72_F_HM) that were used for pathogenicity tests will make a good set of control when the same germplasm is used.

The variation in response of finger millet genotypes to the two isolates tested in this study suggests different levels of cultivar resistance/susceptibility. Our preliminary results indicate that the different isolates are likely to elicit different host reactions in the field. This calls for isolate specific characterization of *MoE* in the future in order to ensure that resistant genotypes are developed based on the predominant virulent isolate in the target regions. Further variation analysis for the rest of the isolates would be necessary to establish their differences and infer on the population structure of the isolates from Kenya. Diversity of the pathogen is attributed to horizontal gene transfer, natural and stress-induced transposition (Chadha and Gopalakrishna 2005). Reports of genotype variations in their response to blast disease have been reported in previous studies in Kenya (Dida et al. 2021; Manyasa et al. 2019; Wekesa et al. 2019). The selected set of 18 diverse genotypes will need to be refined further based on their responses to different isolates. Blast is considered the most destructive fungal disease of finger millet and better understanding of the pathogenicity of distinct isolates will be important to guide breeders in the development of broad-spectrum and durable blast-resistant varieties.

This study demonstrated the need to use more than one method to correctly identify blast isolates collected from symptomatic finger millet grown across different regions of Kenya. Our results have significant implications for the finger millet community based on the differences observed in the pathogen and the host. The information generated in the present study should be exploited in the future to enable comprehensive genetic diversity analysis of isolates from different regions and the characterization of potential pathotypes. The distinctness of the confirmed 46 *MoE* isolates in their pathogenicity will need to be tested as baseline for future pathogen evolution studies, in the same way that has been done in other major crops such as rice and wheat.

Conclusions

This study demonstrated the existence of morpho-cultural and genetic variation among isolates collected from different finger millet growing counties of Kenya. Our results have significant implications for the finger millet community based on the differences observed in the pathogen and the host. The information generated in the present study should be exploited in the future development of breeding strategies to manage finger millet blast disease. The distinctness of the confirmed 46 *MoE* isolates in their pathogenicity will need to be tested as baseline for future pathogen evolution studies, in the same way that has been done in other major crops such as rice and wheat.

Supplementary Information The online version contains supplementary material available at https://doi.org/10.1007/s42161-026-02330-9.

Acknowledgements We acknowledge the support received through the project "Safeguarding crop diversity for food security: Pre-breeding complemented with Innovative Finance", which was funded by the Templeton World Charity Foundation, Inc. (TWCF0400) and the initiative "Adapting Agriculture to Climate Change: Collecting, Protecting and Preparing Crop Wild Relatives", supported by the Government of Norway (QZA-14/0005).

Author contributions DAO, ANW, ENN, EKM and BK conceived the research. ANW, MA, MMD collected the symptomatic samples in the field. ANW, MA and SC performed the laboratory experiments. DAO, ANW, ENN and EKM analysed the results and wrote the initial manuscript draft. DAO, ANW, ENN, EKM and BK contributed in revision of the draft. All authors approved the final draft of the manuscript.

Data availability The datasets generated during and/or analysed in the current study are available from the corresponding author on reasonable request.

Declarations

Ethical approval Not applicable.

Competing interests The authors declare that they have no conflicts of/competing interests.

Open Access This article is licensed under a Creative Commons Attribution-NonCommercial-NoDerivatives 4.0 International License, which permits any non-commercial use, sharing, distribution and reproduction in any medium or format, as long as you give appropriate credit to the original author(s) and the source, provide a link to the Creative Commons licence, and indicate if you modified the licensed material. You do not have permission under this licence to share adapted material derived from this article or parts of it. The images or other third party material in this article are included in the article's Creative Commons licence, unless indicated otherwise in a credit line to the material. If material is not included in the article's Creative Commons licence and your intended use is not permitted by statutory regulation or exceeds the permitted use, you will need to obtain permission directly from the copyright holder. To view a copy of this licence, visit http://creativecommons.org/licenses/by-nc-nd/4.0/.

References

Abed-Ashtiani F, Kadir J, Nasehi A, Hashemian-Rahaghi SR, Vadamalai G, Rambe SK (2016) Characterisation of *Magnaporthe oryzae* isolates from rice in peninsular Malaysia. Czech J Genetic Plant Breed 52(4):145–156

Altschul SF, Gish W, Miller W, Myers EW, Lipman DJ (1990) Basic local alignment search tool. J Mol Biol 215(3):403–410

Aravind K, Rajeswari B, Babu TK, Pushpavalli SNCVL (2022) Pathogenic and molecular variability of *Magnaporthe oryzae* isolates collected from major rice growing locations of Telangana State, India. Indian Phytopathol 75:661–671

Aruna J, Kumar SV, Rambabu R, Ramesh S, Yashaswini C, Bhaskar B, Madhavi KR, Balachndran SM, Ravindrababu V, Prasad MS (2016) Morphological characterization of five different isolates of *Pyricularia oryzae* causing rice blast disease. Int J Soc Sci Dev Agric Technol 11:3377–3380

Babu TK, Thakur RP, Upadhyaya HD, Reddy PN, Sharma R, Girish AG, Sarma NDRK (2013) Resistance to blast (Magnaporthe grisea) in a mini-core collection of finger millet germplasm. Eur J Plant Pathol 135(2):299–311

Chadha S, Gopalakrishna T (2005) Genetic diversity of Indian isolates of rice blast pathogen (*Magnaporthe grisea*) using molecular markers. Curr Sci 88(9):1466–1469

Chen L, Yan W, Wang T, Wang Y, Liu J, Yu Z (2021) Analysis of small and large subunit *r*DNA introns from several ectomycorrhizal fungi species. PLoS ONE 16(3):e0245714

Coelho L, Borrero C, Bueno-Pallero FA, Guerrero C, Fonseca F, Reis M, Avilés M, Dionísio L (2020) First report of *Curvularia trifolii* causing *Curvularia* blight in *Agrostis stolonifera* in south of Portugal. Plant Dis 104(1):292–292

Dida MM, Oduori CA, Manthi SJ, Avosa MO, Mikwa EO, Ojulong HF, Odeny DA (2021) Novel sources of resistance to blast disease in finger millet. Crop Sci 61(1):250–262

Dodds PN, Rathjen JP (2010) Plant immunity: Towards an integrated view of plant–pathogen interactions. Nat Rev Genet 11(8):539–548

Ekwamu A (1991) Influence of head blast infection on seed germination and yield components of finger millet (*Eleusine coracana* L. Gaertn). Trop Pest Manage 37:122–123

Falloon RE (1976) *Curvularia trifolii* as a high-temperature turf grass pathogen. New Z J Agricultural Res 19(2):243–248

Farman M, Peterson G, Chen L, Starnes J, Valent B, Bachi P, Murdock L, Hershman D, Pedley K, Fernandes JM, Bavaresco J (2017) The *Lolium* pathotype of *Magnaporthe oryzae* recovered from a single blasted wheat plant in the United States. Plant Dis 101(5):684–692

Farooq S, Rather TR, Bhat FA, Jan S, Ahangar MA (2023) First report of sunflower leaf spot caused by *Curvularia lunata* under temperate conditions of Kashmir, India. SKUAST J Res 25(4):637–639

Ferdinandez HS, Manamgoda DS, Udayanga D, Deshappriya N, Munasinghe MS, Castlebury LA (2021) Molecular phylogeny and morphology reveal three novel species of *Curvularia (Pleosporales, Pleosporaceae)* associated with cereal crops and weedy grass hosts. Mycological Progress 20:431–451

Gladieux P, Zhang XG, Roldan-Ruiz I, Caffier V, Leroy T, Devaux M, Van Glabeke S, Coart E, Le Cam B (2010) Evolution of the population structure of *Venturia inaequalis*, the apple scab fungus, associated with the domestication of its host. Mol Ecol 19:658–674

Gowda M, Shirke MD, Mahesh HB, Chandarana P, Rajamani A, Chattoo BB (2015) Genome analysis of rice-blast fungus *Magnaporthe oryzae* field isolates from southern India. Genomics data 5:284–291

Grovermann C, Umesh KB, Quiédeville S, Kumar BG, Moakes S (2018) The economic reality of underutilised crops for climate resilience, food security and nutrition: Assessing finger millet productivity in India. Agriculture 8(9):131

Gupta DR, Surovy MZ, Mahmud NU, Chakraborty M, Paul SK, Hossain MS, Bhattacharjee P, Mehebub MS, Rani K, Yeasmin R, Rahman M, Islam MT (2020) Suitable methods for isolation, culture, storage and identification of wheat blast fungus *Magnaporthe oryzae Triticum* pathotype. Phytopathol Res 2(1):30

Hall TA (1999) BioEdit: A user-friendly biological sequence alignment editor and analysis program for Windows 95/98/NT. Nucleic Acids Symp Ser 41(41):95–98

Harmon PF, Dunkle LD, Latin R (2003) A rapid PCR-based method for the detection of *Magnaporthe oryzae* from infected perennial ryegrass. Plant Dis 87(9):1072–1076

He J, Li DW, Cui WL, Huang L (2024) Seven new species of *Alternaria (Pleosporales, Pleosporaceae)* associated with Chinese fir, based on morphological and molecular evidence. MycoKeys 2101:1

Hilu KW, De Wet JM (1976) Domestication of *E. coracana*. Econ Bot 30:199–208

Hirata K, Kusaba M, Chuma I, Osue J, Nakayashiki H, Mayama S, Tosa Y (2007) Speciation in *Pyricularia* inferred from multilocus phylogenetic analysis. Mycol Res 111(7):799–808

Jia Y, Lee FN, McClung A (2009) Determination of resistance spectra of the Pi-ta and Pi-k genes to US races of Magnaporthe oryzae causing rice blast in a recombinant inbred line population. Plant Dis 93(6):639–644

Kachroo P, Leong SA, Chattoo BB (1994) *Pot2*, an inverted repeat transposon from the rice blast fungus *Magnaporthe grisea*. Mol Gen Genet 245(3):339–348

Kang H, Peng Y, Hua K, Deng Y, Bellizzi M, Gupta DR, Mahmud NU, Urashima AS, Paul SK, Peterson G (2021) Rapid detection of wheat blast pathogen *Magnaporthe oryzae Triticum* pathotype using genome-specific primers and Cas12a-mediated technology. Engineering 7(9):1326–1335

Kato H, Yamamoto M, Yamaguchi-Ozaki T, Kadouchi H, Iwamoto Y, Nakayashiki H, Tosa Y, Mayama S, Mori N (2000) Pathogenicity, mating ability and DNA restriction fragment length polymorphisms of *Pyricularia* populations isolated from *Gramineae, Bambusideae* and *Zingiberaceae* plants. J Gen Plant Pathol 66:30–47

Kumar S, Stecher G, Li M, Knyaz C, Tamura K (2018) MEGA X: Molecular evolutionary genetics analysis across computing platforms. Mol Biol Evol 35(6):1547–1549

Longya A, Talumphai S, Jantasuriyarat C (2020) Morphological characterization and genetic diversity of rice blast fungus, *Pyricularia oryzae*, from Thailand using ISSR and SRAP markers. J Fungi 6(1):38

Mahamadou D, Adounigna K, Amadou HB, Oumarou H, Fousseyni C, Abdoulaye H (2022) Isolation and in-vitro assessment of antagonistic activity of Trichoderma spp. against Magnaporthe oryzae Longorola strain causing rice blast disease in Mali. Afr J Microbiol Res 16(2):67–75

Manyasa EO, Tongoona P, Shanahan P, Githiri S, Ojulong H, Njoroge SM (2019) Exploiting genetic diversity for blast disease resistance sources in finger millet (*Eleusine coracana*). Plant Health Progress 20(3):180–186

Meena BS (2005) Morphological and molecular variability of rice blast pathogen *Pyricularia grisea* (Cooke) Sacc. M.Sc. Thesis. Dharwad. University of Agricultural Sciences, Dharwad

Muni NM, Nadarajah K (2014) Morphological and molecular characterization of *Magnaporthe oryzae* (fungus) from infected rice leaf samples. In AIP Conference Proceedings 1614(1):756–760

Muthomi JW, Mutitu EW (2003) Occurrence of mycotoxin producing Fusarium species and other fungi on wheat kernels harvest in selected districts of Kenya. Afr Crop Sci Conf Proc 6:335–339

Noman M, Al A, Hosen S, Shamsi S (2022) Elucidating genetic diversity and population structure of Pyricularia oryzae isolates causing wheat blast in Bangladesh. Arch Microbiol 204:1–10

Odeny DA, Niazi A, Tesfaye K, Lule D, Wanyonyi S, Kunguni JS (2020) Genomic designing for climate smart finger millet. Genomic Designing Climate-Smart Cereal Crops, 287–307

Odeph M, Kavoo A, Mweu C, Mbinda W (2021) Identification and characterization of fungal species associated with the finger millet pathogen *Pyricularia oryzae* in Kenya. J Plant Pathol 103(4):1153–1167

Palanna KB, Vinaykumar HD, Koti PS, Jeevan B, Rajashekara H, Raveendra HR, Patro TSSK, Ramesh GV, Mudalagiriyappa, Rawat L, Netam P, Ekka S, Rajesha G, Das IK, Chandranayaka S, Nagaraja TE, Satyavathi CT (2024) Geographic distribution, host preference and phylogenetic relationships among *Pyricularia* species inciting millet and rice blast disease in India. Plant Pathol 73(3):692–705

Palanna KB, Vinaykumar HD, Prasanna SK, Rajashekara H, Devanna BN, Anilkumar C, Jeevan B, Raveendra HR, Khan F, Bhavana CS, Upadhyay V (2023) Exploring the diversity of virulence genes in the *Magnaporthe* population infecting millets and rice in India. Front Plant Sci 9(14):1131315

Panda G, Sahu C, Yadav MK, Aravindan S, Umakanta N, Raghu S, Prabhukarthikeyan SR, Lenka S, Tiwari JK, Kar S (2017) Morphological and molecular characterization of *Magnaporthe oryzae* from Chhattisgarh. ORYZA-An Int J Rice 54(3):330–336

Pereira JF, Consoli L, de Souza Bombonatto EA, Bonato AL, Maciel JL (2014) Development of genomic SSR markers and molecular characterization of *Magnaporthe oryzae* isolates from wheat in Brazil. Biochem Genet 52:52–70

Pieck ML, Ruck A, Farman ML, Peterson GL, Stack JP, Valent B, Pedley KF (2017) Genomics-based marker discovery and diagnostic assay development for wheat blast. Plant Dis 101(1):103–109

Prakash G, Srinivasa N, Sankar SM, Singh SP, Satyavathi CT (2016) Standardization of pearl millet blast (*Magnaporthe grisea*) phenotyping under artificial conditions. Ann Agric Res 37(2)

Puri S, Kumar J (2012) Characterization of leaf, neck and finger blast pathogen populations from *Eleusine coracana* and elucidating their interrelationships in *Eleusine-Magnaporthe* pathosystem. Indian Phytopathol 65(2):133

Rajashekara H, Prakash G, Pandian RTP, Sarkel S, Dubey A, Mishra D, Sharma P, Sharma TR, Singh UD (2016 Feb) A selective method and media for single spore isolation of Magnaporthe spp. From blast infected samples. IPS 6th International Conference on Plant, Pathogens, People 23–27, New Delhi:238

Rao ANS (1990) Estimates of losses in finger millet (*Eleusine coracana*) due to blast disease (*Pyricularia grisea*)

Sahu C, Yadav MK, Panda G, Aravindan S, Umakanta N, Raghu S, Prabhukarthikeyan SR, Keerthana U, Adak T, Sharma V, Mohanty MR (2018) Morphological and molecular characterization of *Magnaporthe oryzae* causing rice blast disease in Odisha. ORYZA-An Int J Rice 55(3):467–472

Saleh D, Milazzo J, Adreit H, Fournier E, Tharreau D (2014) South-East Asia is the center of origin, diversity and dispersion of the rice blast fungus, *Magnaporthe oryzae*. New Phytology 201:1440–1456

Sansaloni C, Petroli C, Jaccoud D, Carling J, Detering F, Grattapaglia D, Kilian A (2011) Diversity Arrays Technology (DArT) and next-generation sequencing combined: genome-wide, high throughput, highly informative genotyping for molecular breeding of Eucalyptus. BMC Proc 5:P54. https://doi.org/10.1186/1753-6561-5-S7-P54

Schoch CL, Seifert KA, Huhndorf S, Robert V, Spouge JL, Levesque CA, Chen W, Bolchacova E, Voigt K, Crous PW, Miller AN, Wingfield MJ, Aime MC, An KD, Bai FY, Barreto RW, Begerow D, Schindel D (2012) Nuclear ribosomal internal transcribed spacer (ITS5/4) region as a universal DNA barcode marker for Fungi. Proc Natl Acad Sci United States 109(16):6241–6246

Shi X, Zhang S, Yang Y, Jia L, Herrera-Balandrano DD, Wang S, Laborda P (2024) Occurrence and management of the emerging pathogen *Epicoccum sorghinum*. Plant Disease

Taguiam JD, Evallo E, Balendres MA (2021) *Epicoccum* species: ubiquitous plant pathogens and effective biological control agents. Eur J Plant Pathol 159:713–725

Takan JP, Chipili J, Muthumeenakshi S, Talbot NJ, Manyasa EO, Bandyopadhyay R, Sere Y, Nutsugah SK, Talhinhas P, Hossain M (2012) *Magnaporthe oryzae* populations adapted to finger millet and rice exhibit distinctive patterns of genetic diversity, sexuality and host interaction. Mol Biotechnol 50:145–158

Tembo B, Mulenga RM, Sichilima S, M'siska KK, Mwale M, Chikoti PC, Singh PK, He X, Pedley KF, Peterson GL, Singh RP (2020) Detection and characterization of fungus (*Magnaporthe oryzae* pathotype *Triticum*) causing wheat blast disease on rain-fed grown wheat (*Triticum aestivum L.*) in Zambia. PLoS ONE 15(9):e0238724

Terensan S, Fernando HNS, Silva JN, Perera SACN, Kottearachchi NS, Weerasena OVDSJ (2022) Morphological and molecular analysis of fungal species associated with blast and brown spot diseases of *Oryza sativa*. Plant Dis 106(6):1617–1625

Vanaraj P, Kandasamy S, Ambalavanan S, Ramalingam R, Sabariyappan R (2013) Variability in *Pyricularia oryzae* from different rice growing regions of Tamil Nadu, India. Afr J Microbiol Res 7(26):3379-88

Wekesa CM, Kimurto PK, Oduori CO, Towett BK, Jeptanui L, Ojulong H, Siambi M (2019) Sources of resistance to blast disease (*Pyricularia grisea* L.) in finger millet (*Eleusine Coracana*) germplasm. J Life Sci 13(1):34–47

Xing J, Jia Y, Peng Z, Shi Y, He Q, Shu F, Zhang W, Zhang Z, Deng H (2017) Characterization of molecular identity and pathogenicity of Rice blast fungus in Hunan Province of China. Plant Dis 101(4):557–561

Zhang H, Hall N, Goertzen LR, Chen CY, Peatman E, Patel J, McElroy JS (2019) Transcriptome analysis reveals unique relationships among *Eleusine* species and heritage of *Eleusine coracana*. G3-Genes Genomes Genetics 9(6):2029–2036

Publisher's note Springer Nature remains neutral with regard to jurisdictional claims in published maps and institutional affiliations.